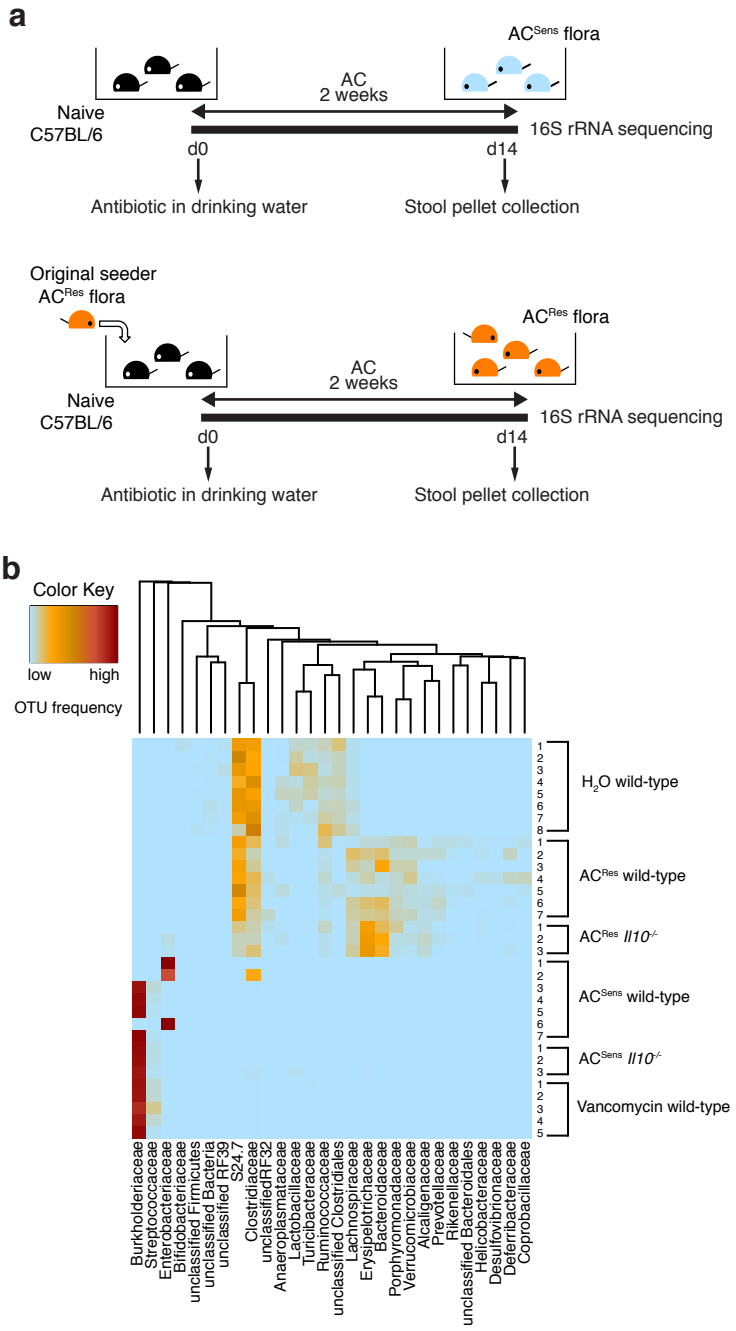

Supplementary Figure 1 *In vivo* model of intestinal dysbiosis and antibiotic-resistant flora. (**a**) Upper panel, experimental layout of intestinal dysbiosis. Experimental naive 7-week-old C57BL/6 mice are treated for 2 weeks with amoxicillin and clavulanic acid (AC). Mice with a modification of the intestinal microbiota are named AC-sensitive flora mice (AC^{Sens}). Lower panel, colonization of AC resistant flora (AC^{Res}) from the original seeder mouse to naive 7-week-old C57BL/6 mice. Naive mice (black) are co-housed with a seeder mouse (orange) carrying antibiotic resistant microbiota and received antibiotics in the drinking water for 2 weeks. Because of the coprophagic behavior of mice, the resistant flora is successfully transmitted to naive mice. Stool pellets are collected 14 days after co-housing for 16S ribosomal RNA (rRNA) analysis. (**b**) The heat map depicts family-level operational taxonomic unit (OTU) frequencies of bacterial populations observed in non-treated animals (H_2O), AC^{Res}, AC^{Sens} wild-type and *Il10*$^{-/-}$ KO mice, and vancomycin-treated wild-type mice after 2 weeks of treatment. Only OTUs with frequency > 1% were included.

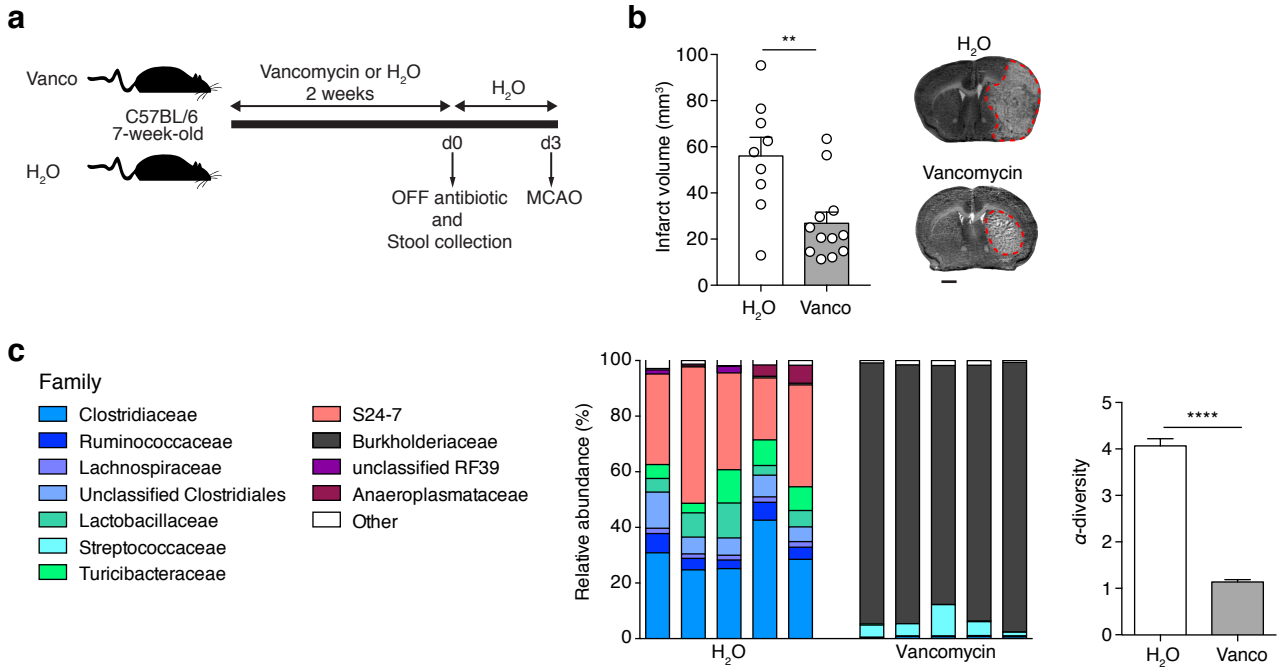

Supplementary Figure 2 Vancomycin alters gut flora and induces protection from ischemic brain injury. (**a**) Experimental layout of vancomycin treatment in 7-week-old C57BL/6 mice. Mice receive water alone (H_2O) or vancomycin (Vanco) in drinking water (0.5 g/L) for 2 weeks. Stool pellets are collected 14 days after treatment for r16S sequencing. Administration of antibiotic is discontinued 3 days prior to MCAO. (**b**) Infarct volume of H_2O ($n = 9$) and vancomycin ($n = 12$) mice as measured by Nissl staining of brain sections on day 3 post MCAO (bar, 1 mm). (**c**) Left panel indicates color code for the most predominant bacterial families found in the mouse intestine. Mid panel shows phylogenetic classification of 16S rDNA frequencies in stool samples collected from H_2O and vancomycin mice treated for 2 weeks. Each bar represents one mouse. Right panel depicts intestinal microbiota α-diversity (H_2O, $n = 8$; vancomycin, $n = 5$). Throughout, error bars represent mean ± s.e.m. $^{**}P < 0.01$, $^{****}P < 0.0001$; by Student's *t*-test.

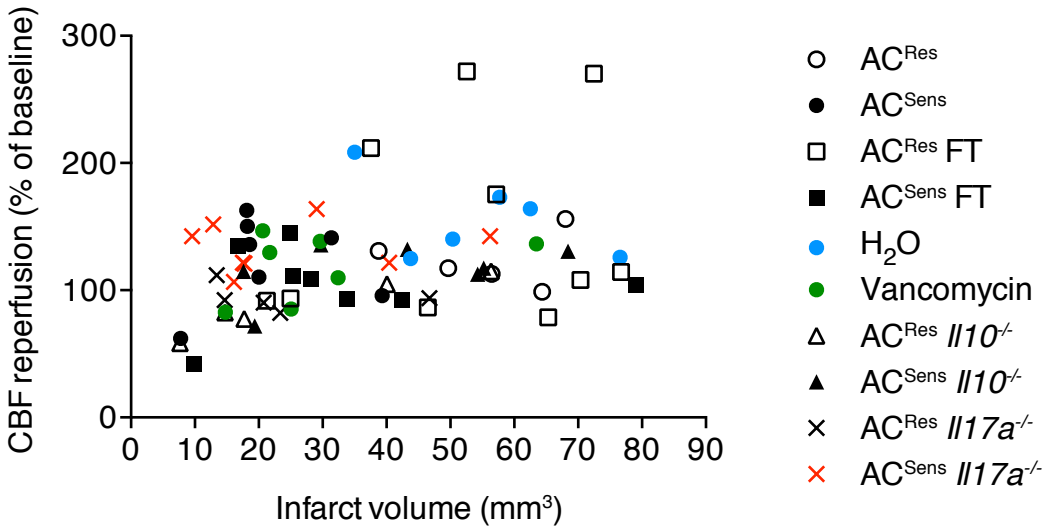

Supplementary Figure 3 Correlation plot between cerebral blood flow (CBF) reperfusion (mean values are from 10 to 20 minutes after reperfusion) and infarct volume 72 h after MCAO in all groups tested; each data point represent one animal.

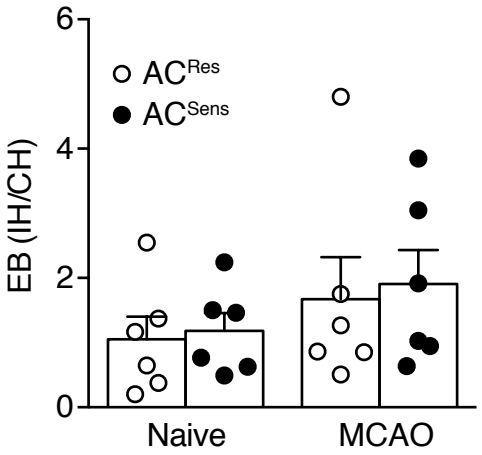

Supplementary Figure 4 Measurement of blood brain barrier permeability by Evans Blue (EB) extravasation is not different in naive AC^{Res} and AC^{Sens} mice and 6 h after MCAO. Data are expressed as ratio of the ipsilateral hemisphere (IH) and contralateral hemisphere (CH), (n = 6 per group). Columns represent mean ± s.e.m. (Student's t-test).

Benakis *et al.* Supplementary Figure 5

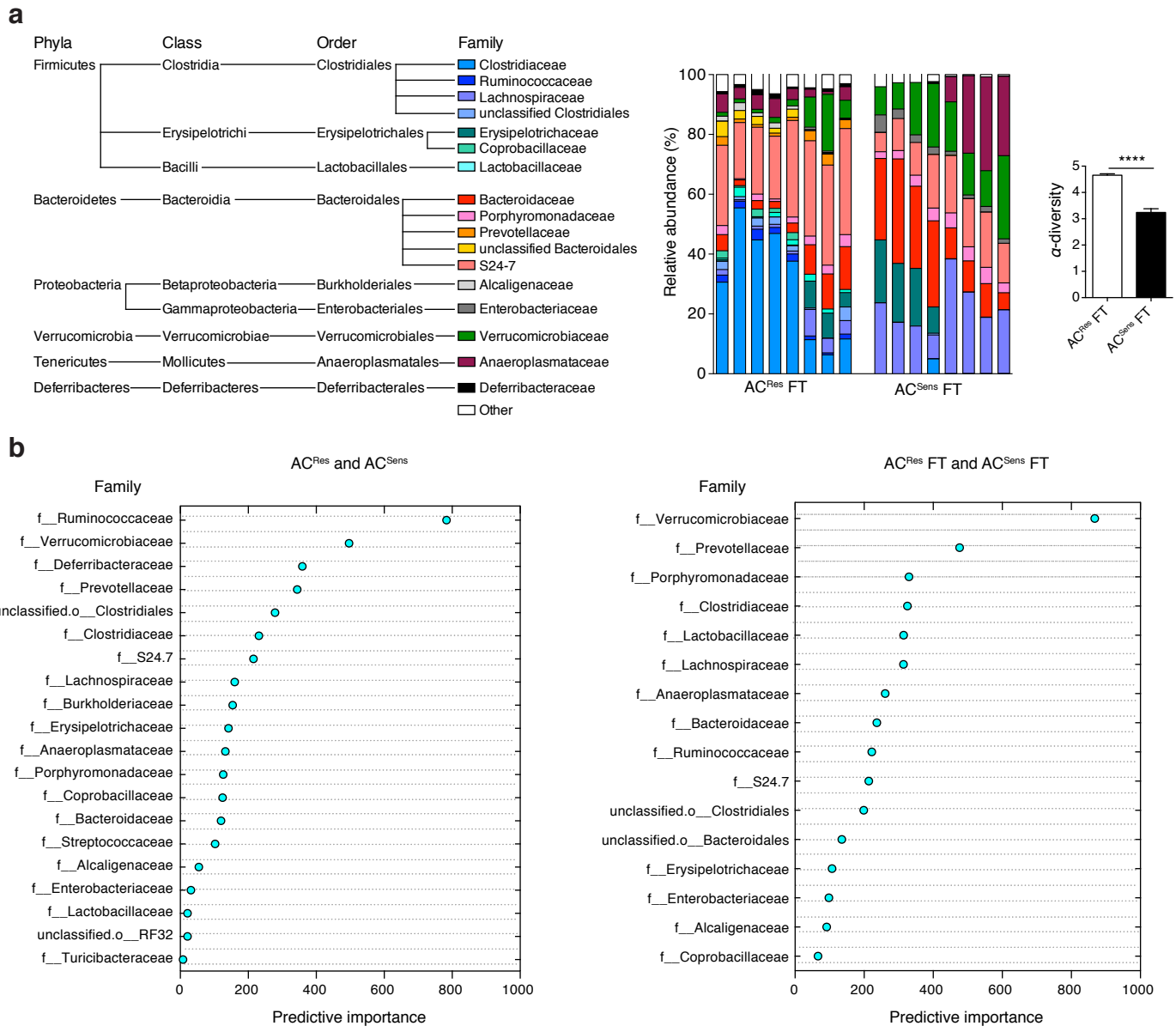

Supplementary Figure 5 Phylogenetic analysis of fecal transplanted (FT) mice. (**a**) Left panel indicates color code for the most predominant bacterial families. Mid panel shows family-level phylogenetic classification of 16S rDNA frequencies in stool samples collected from AC^{Res} and AC^{Sens} mice 2 weeks after fecal transplantation. Each bar represents an individual animal. For clarity only families represented over 1% were included. Right, graph depicts intestinal microbiota *α*-diversity ($n = 8$ per group). Columns represent mean ± s.e.m. ****$P < 0.0001$ (Student's *t*-test). (**b**) Random forest analysis showing predictive importance of operational taxonomic units (OTU) at the family level (OTUs > 1% were included) trained for stroke outcome in AC^{Res} and AC^{Sens} (left panel) and AC^{Res} FT and AC^{Sens} FT mice (right panel).

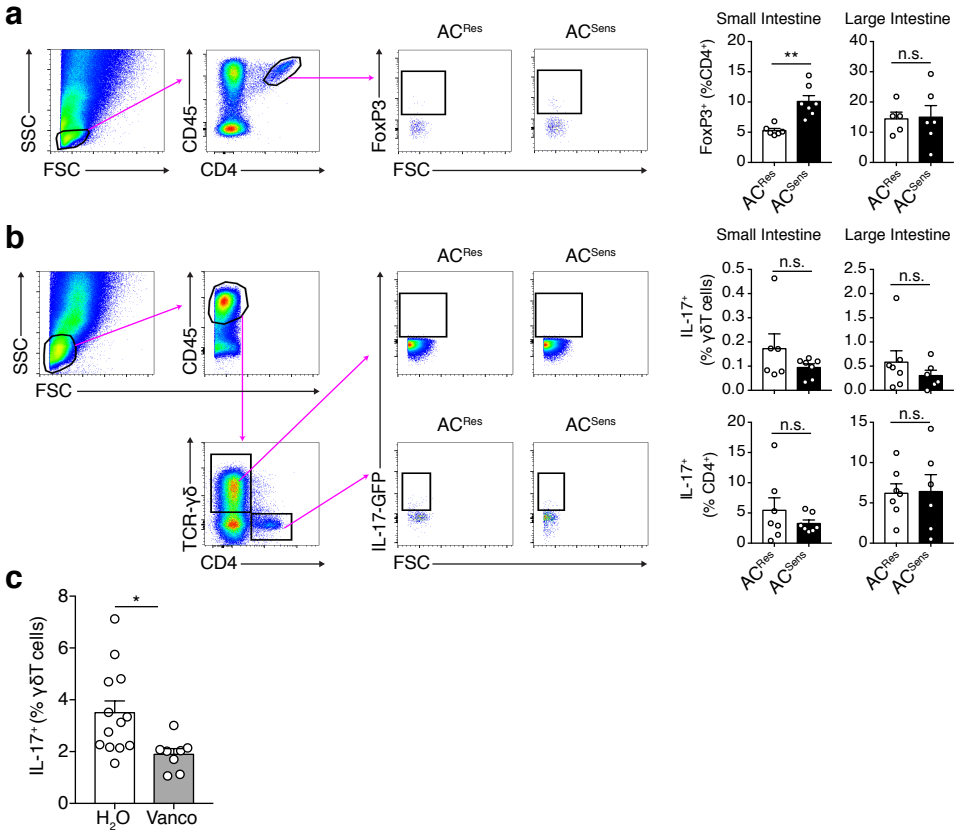

Supplementary Figure 6 T_{reg}, but not IL-17⁺ γδ T cells are affected in intraepithelial lymphocytes (IELs) of AC^{Sens} mice. (**a**) T_{reg} population ($CD45^+CD4^+FoxP3^+$) in the IELs of the small intestine of AC^{Res} and AC^{Sens} analyzed by flow cytometry. Graphs represent percentage of $FoxP3^+$ in the epithelium of the small (AC^{Res}, $n = 6$ and AC Sens, $n = 7$) and large intestine (AC^{Res}, $n = 5$ and AC^{Sens}, $n = 6$). (**b**) Flow cytometry analyzing IL-17 production in γδ T cells ($CD45^+TCR\text{-}\gamma\delta^+CD4^-$) and T_H17 ($CD45^+TCR\text{-}\gamma\delta^-CD4^+$) in the IELs of the small intestine from AC^{Res} and AC^{Sens} mice after two weeks on antibiotic. The boxes in the dot plots gate IL-17⁺ cells in γδ T cells (first row) and IL-17⁺ in T_H17 cells (second row) in AC^{Res} and AC^{Sens} mice. The bar graphs indicate percentage of IL-17 producing cells in the small (AC^{Res}, $n = 6$–7 and AC^{Sens}, $n = 7$) and large intestine (AC^{Res}, $n = 7$ and AC Sens, $n = 6$). Columns represent mean ± s.e.m.; no significant changes (n.s.) are observed between groups (Student's *t*-test). (**c**) Similarly to AC treatment, IL-17⁺ γδ T cells are suppressed in the lamina propria (LP) of the small intestine in vancomycin-treated mice. Graphs show percentage of IL-17 production in γδT cells ($CD45^+TCR\text{-}\gamma\delta^+CD4^-$) in the LP of the small intestine from H_2O ($n = 13$) and vancomycin ($n = 8$) mice after 2 weeks. Columns represent mean ± s.e.m. $^*P < 0.05$ and $^{**}P < 0.01$ (Student's *t*-test).

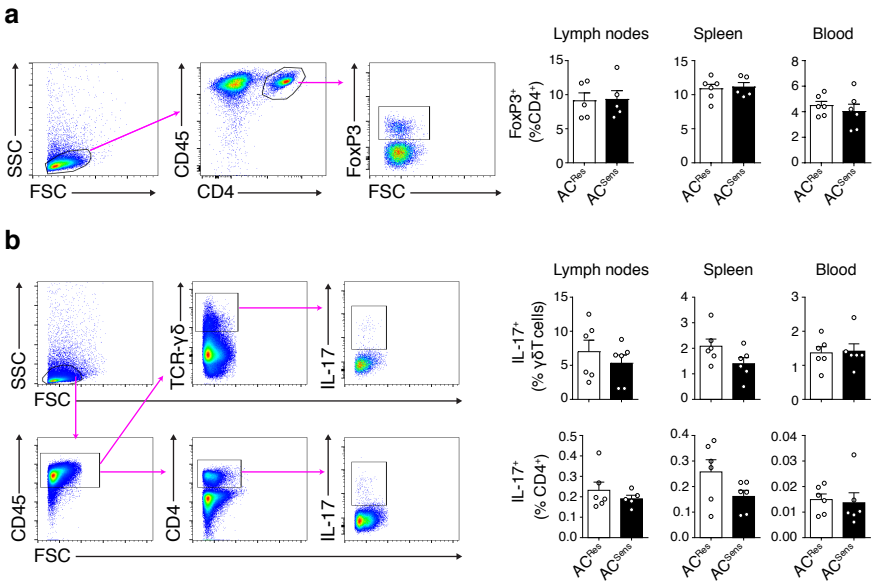

Supplementary Figure 7 IL-17$^+$ γδ T cells, IL-17$^+$ CD4 cells (T_H17) and T_{reg} cell analysis in lymph nodes, spleen and blood of AC^{Res} and AC^{Sens} mice. (**a**) Flow cytometry gating strategy of T_{reg} cells (CD45$^+$CD4$^+$FoxP3$^+$) in the lymph nodes. Graphs indicate number of FoxP3$^+$ cells as a percentage of CD4$^+$ cells in AC^{Res} and AC^{Sens} mice in the lymph nodes ($n = 5$ per group), spleen (AC^{Res}, $n = 6$ and AC^{Sens}, $n = 5$) and blood ($n = 6$ per group). (**b**) Flow cytometry gating strategy to identify IL-17$^+$ γδ T cells (CD45$^+$TCR-γδ$^+$IL-17$^+$) and T_H17 cells (CD45$^+$CD4$^+$IL-17$^+$) in the lymph nodes. IL-17 production is analyzed by intracellular staining of IL-17. Graphs indicate number of IL-17$^+$ cells as a percentage of γδ T cells (first row) and IL-17$^+$ cells as a percentage of CD4 cells (second row) in AC^{Res} and AC^{Sens} mice in the lymph nodes, spleen and blood ($n = 6$ per group). Throughout, error bars represent mean ± s.e.m.; no significant changes are observed between groups (Student's *t*-test).

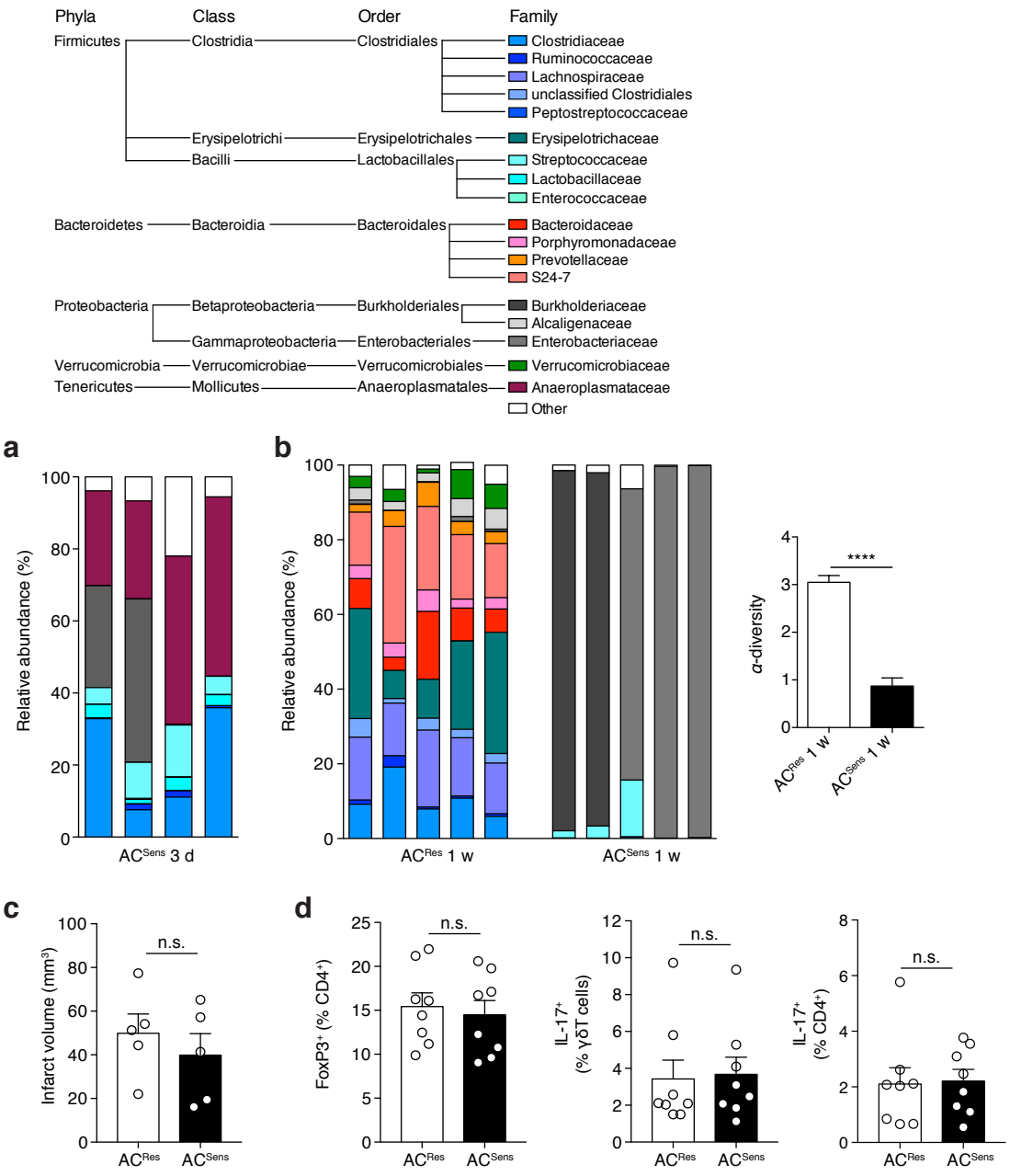

Supplementary Figure 8 One week of AC treatment does not induce protection from ischemic brain injury and changes in intestinal immune cell response. Top panel indicates color code for the most predominant bacterial families. Lower panel shows family-level phylogenetic classification of 16S rDNA frequencies in stool samples collected (**a**) from AC^{Sens} mice treated for 3 days or (**b**) from AC^{Res} and AC^{Sens} after 1 week of antibiotic. Each bar represents an individual animal. Only families represented over 1% were included. Right, graph depicts intestinal microbiota *α*-diversity ($n = 4–5$). (**c**) Infarct volume of AC^{Res} ($n = 5$) and AC^{Sens} ($n = 5$) mice treated for 1 week as measured by Nissl staining of coronal brain sections on day 3 post MCAO (bar, 1 mm). (d) Flow cytometry analyzing T_{reg} (CD45$^+$CD4$^+$FoxP3$^+$), IL-17 production in γδ T cells (CD45$^+$TCR-γδ$^+$CD4$^-$) and T_H17 cells (CD45$^+$TCR-γδ$^-$CD4$^+$) in the LP of the small intestine from AC^{Res} and AC^{Sens} mice after 1 week on antibiotic ($n = 8$ per group). Data are expressed as mean ± s.e.m. ****$P < 0.0001$; n.s., not significant; by Student's *t*-test.

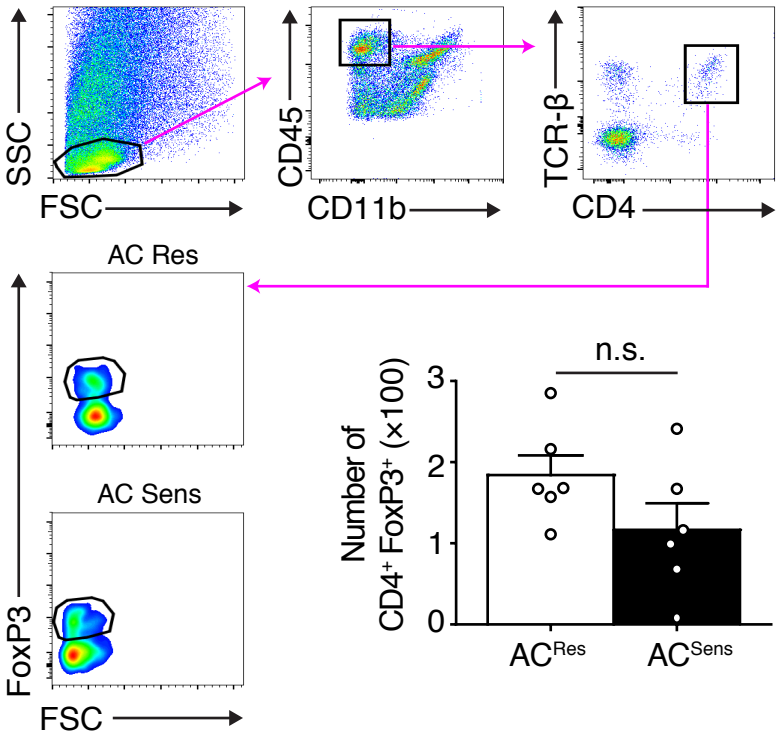

Supplementary Figure 9 Intestinal dysbiosis does not alter meningeal T_{reg} after brain ischemia. Flow cytometry analyzing regulatory T cells ($CD45^{high}CD4^{+}TCR\text{-}\beta^{+}FoxP3^{+}$) in the meninges of AC^{Res} and AC^{Sens} mice 16 h after ischemia. The graph represents the total number of meningeal T_{reg} 16 h after MCAO in AC^{Res} ($n = 6$) and AC^{Sens} ($n = 6$) mice. One data point represent one animal. Columns represent mean ± s.e.m.; n.s., not significant (Student's *t*-test).

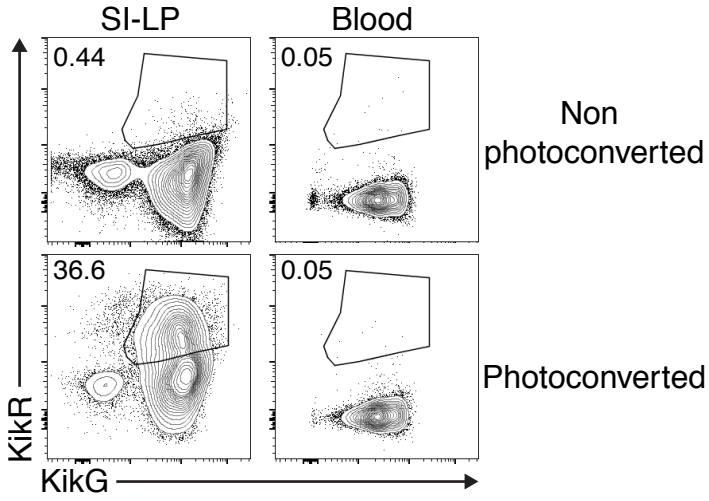

Supplementary Figure 10 Photoconversion in the small intestine does not label circulating immune cells. Distal small intestine (6 cm) from KikGR mice are exposed for 20 min to violet light (405 nm) (photoconverted) or to ambient room light (non-photoconverted). Immediately after photoconversion, blood and small intestine (SI-LP) are extracted and analyzed by flow cytometry for $KikR^+$ cells. The gates in the dot plots identify $KikR^+$ cells, and the numbers are the percentage of $KikR^+$ cells of total lymphocytes ($CD45^{high}CD11b^-$); gating strategy is as indicated in Figure 4b.

	CBF MCA occlusion (%)	CBF reperfusion (%)	week old	weight (g)	body temperature (°C)	N	protection (+/-)
AC^{Res}	8.1 ± 0.7	126.5 ± 9.2	9.4 ± 0.07	25.3 ± 0.3	36.6 ± 0.1	16	-
AC^{Sens}	10.2 ± 1.1	132.5 ± 8.2	9.4 ± 0.06	24.3 ± 0.4	35.7 ± 0.4	18	+
AC^{Res} FT	9.6 ± 0.9	150.2 ± 24.2	9.3 ± 0.09	22.7 ± 0.6**	35.6 ± 0.2	10	-
AC^{Sens} FT	9.1 ± 1.0	102.6 ± 9.9	9.2 ± 0.10	23.3 ± 0.5	35.8 ± 0.2	9	+
H_2O	11.4 ± 0.9	165.2 ± 14.4	9.3 ± 0.02	23.6 ± 0.7	35.8 ± 0.2	7	-
Vancomycin	8.1 ± 0.7	118.5 ± 9.9	9.4 ± 0.01	24.8 ± 0.5	35.8 ± 0.2	7	+
AC^{Res} *Il10*$^{-/-}$	6.9 ± 0.4	87.6 ± 10.1∞	9.2 ± 0.06	23.9 ± 0.6	36.2 ± 0.3	5	-
AC^{Sens} *Il10*$^{-/-}$	7.6 ± 0.8	116.5 ± 8.2	9.3 ± 0.06	24.3 ± 0.4	36.1 ± 0.3	7	-
AC^{Res} *Il17a*$^{-/-}$	9.1 ± 0.9	94.0 ± 4.9	9.6 ± 0.2	22.5 ± 1.0*	35.7 ± 0.1	5	+
AC^{Sens} *Il17a*$^{-/-}$	10.0 ± 1.3	133.9 ± 6.8	9.3 ± 0.1	24.0 ± 0.7	36.1 ± 0.3	8	+

Supplementary Table 1 Percentages of cerebral blood flow (CBF) reduction after middle cerebral artery (MCA) occlusion and CBF mean values from 10 to 20 min after reperfusion. Mouse age (weeks), weight (g) and body temperature (°C) at the time of MCAO induction. Data are represented as mean ± s.e.m. ∞ indicate significant difference in CBF reperfusion between H_2O and AC^{Res} *Il10*$^{-/-}$ mice, ∞p<0.05 (one-way ANOVA), and * indicate significant difference in body weight between AC^{Res}, and AC^{Res} FT and AC^{Res} *Il17a*$^{-/-}$, *P < 0.05 and **P < 0.01 (one-way ANOVA).

	N	exclusion (death)	exclusion (CBF)	survival 72 h post MCAO(%)
AC^{Res} (Fig.1d)	9	1	0	88
AC^{Sens} (Fig.1d)	11	2	0	82
AC^{Res} (Fig.1e)	12	1	0	92
AC^{Sens} (Fig.1e)	14	3	0	79
AC^{Res} FT	10	0	2	100
AC^{Sens} FT	9	0	1	100
H_2O	10	0	1	100
Vancomycin	13	1	0	92
AC^{Res} *Il10*$^{-/-}$	9	2	1	78
AC^{Sens} *Il10*$^{-/-}$	10	1	0	90
AC^{Res} *Il17a*$^{-/-}$	6	0	0	100
AC^{Sens} *Il17a*$^{-/-}$	11	3	0	73

Supplementary Table 2 Number of mice excluded upon death and non-satisfactory cerebral blood flow (CBF) during occlusion or 10 min after reperfusion. The percentage of survival at 72 h after MCAO is not different between groups and treatment (Fisher's exact test).

a

	AC^{Res} microglia			AC^{Sens} microglia			
	mean	s.e.m	n	mean	s.e.m	n	P value
naive	23950	3520	9	23099	3531	8	0.9
d1	36908	2951	6	27742	3405	8	0.1
d2	24299	3128	7	31153	4933	9	0.2
d3	21409	3598	9	19373	1745	9	0.7

	AC^{Res} CD45			AC^{Sens} CD45			
	mean	s.e.m	n	mean	s.e.m	n	P value
naive	1744	316	9	1298	101	8	1.0
d1	4172	1612	6	1708	233	7	0.8
d2	53167	11179	7	17464	5775	9	0.0004
d3	41100	12315	9	7203	1242	7	0.0007

	AC^{Res} mono/mph			AC^{Sens} mono/mph			
	mean	s.e.m	n	mean	s.e.m	n	P value
naive	595	112	9	486	52	8	1.0
d1	2560	1226	6	796	161	7	0.8
d2	26420	8266	7	11382	3126	9	0.0
d3	28605	8535	9	5145	1022	8	0.0004

	AC^{Res} PMN			AC^{Sens} PMN			
	mean	s.e.m	n	mean	s.e.m	n	P value
naive	358	82	9	249	32	8	1.0
d1	566	155	5	394	84	7	0.9
d2	18823	4765	7	1313	279	8	2E-09
d3	4173	1463	9	601	105	7	0.1

	AC^{Res} CD4			AC^{Sens} CD4			
	mean	s.e.m	n	mean	s.e.m	n	P value
naive	70	13	9	74	12	8	1.0
d1	107	47	6	71	17	8	0.7
d2	373	86	7	142	36	9	0.004
d3	481	104	9	109	19	9	3E-06

	AC^{Res} CD8			AC^{Sens} CD8			
	mean	s.e.m	n	mean	s.e.m	n	P value
naive	51	12	9	43	5	8	0.8
d1	56	14	5	64	15	8	0.8
d2	117	22	7	69	16	8	0.2
d3	268	55	9	76	19	9	1E-06

	AC^{Res} B cells			AC^{Sens} B cells			
	mean	s.e.m	n	mean	s.e.m	n	P value
naive	121	38	9	74	20	8	0.3
d1	55	23	6	47	11	8	0.9
d2	165	31	7	86	21	9	0.1
d3	214	65	9	87	19	8	0.011

	AC^{Res} NK			AC^{Sens} NK			
	mean	s.e.m	n	mean	s.e.m	n	P value
naive	1	1	9	0	0	6	0.9
d1	11	5	6	13	5	8	0.9
d2	37	10	7	11	4	8	0.3
d3	82	37	9	25	8	8	0.012

b

	%reduction AC^{Sens} PMN of AC^{Res}	%reduction AC^{Sens} mono/mph of AC^{Res}	%reduction AC^{Sens} CD8 of AC^{Res}	%reduction AC^{Sens} B cells of AC^{Res}	%reduction AC^{Sens} NK of AC^{Res}
n	8	9	8	9	8
mean	-93.02	-56.92	-40.95	-47.74	-69.58
s.e.m	1.484	11.83	13.47	12.67	10.12

Supplementary Table 3 Supportive table to Fig.3a. (**a**) Exact *n* values, absolute number of cells in the ischemic hemisphere (mean ± s.e.m.) and *P* values in AC^{Res} and AC^{Sens} naive mice and days 1, 2 and 3 after MCAO for each immune cell markers analyzed by flow cytometry. Outliers were identified using the ROUT method with a maximum false discovery rate of Q = 2%. (**b**) Exact *n* values and percentages of immune cell reduction 2 days after MCAO (mean ± s.e.m.) in AC^{Sens} mice compared to AC^{Res} mice.

	T_{reg} from WT $CD4^+$ cells induced with $DC\text{-}AC^{Sens}$			T_{reg} from WT $CD4^+$ cells induced with $DC\text{-}AC^{Res}$			T_{reg} from *Il10*$^{-/-}$ $CD4^+$ cells induced with $DC\text{-}AC^{Sens}$		
Ratio T_{reg}/γδT	mean	s.e.m.	n	mean	s.e.m.	n	mean	s.e.m.	n
0:1	100		11	100		14	100		9
1:8	75.26	6.230	11	98.82	5.084	12	107.7	9.673	9
1:4	63.31	6.060	11	91.99	5.995	14	78.80	5.224	9
1:2	54.54	5.404	11	64.82	5.018	13	70.34	8.069	9
1:1	38.24	4.703	11	54.82	4.533	13	56.12	4.703	9

Supplementary Table 4 Supportive tables to Fig.6d showing exact *n* values, percentage of IL-17^+ γδ T cells (mean ± s.e.m.) per group and ratio for each data point analyzed by flow cytometry.